Supplementary Materials

Enhanced Photocatalytic CO_2 Reduction over TiO_2 Using Metalloporphyrin as the Cocatalyst

Ziyi Wang [1,2], Wei Zhou [3], Xin Wang [1,2], Xueliang Zhang [1,2,4], Huayu Chen [1,2], Huilin Hu [1], Lequan Liu [1,2], Jinhua Ye [1,2,5] and Defa Wang [1,2,*]

1 TJU-NIMS International Collaboration Laboratory, Key Lab of Advanced Ceramics and Machining Technology (Ministry of Education), Tianjin Key Lab of Composite and Functional Materials, School of Materials Science and Engineering, Tianjin University, 92 Weijin Road, Tianjin 300072, China; sarah_wangzy@sina.com (Z.W.); xwangtnjrc@tju.edu.cn (X.W.); zhangxueliang@tju.edu.cn (X.Z.); hychen@tju.edu.cn (H.C.); huhuilin@tju.edu.cn (H.H.); lequan.liu@tju.edu.cn (L.L.); jinhua.ye@nims.go.jp (J.Y.)

2 Collaborative Innovation Center of Chemical Science and Engineering (Tianjin), 92 Weijin Road, Tianjin 300072, China

3 Department of Physics, School of Sciences, Tianjin University, 92 Weijin Road, Tianjin 300072, China; weizhou@tju.edu.cn

4 School of Materials and Metallurgical Engineering, Guizhou Institute of Technology, 1 Caiguan Road, Guiyang 550003, China

5 International Center of Materials Nanoarchitectonics (WPI-MANA), National Institute for Materials Science (NIMS), 1-1Namiki, Tsukuba, Ibaraki 305-0044, Japan

* Correspondence: defawang@tju.edu.cn; Tel.: +86-022-27405065

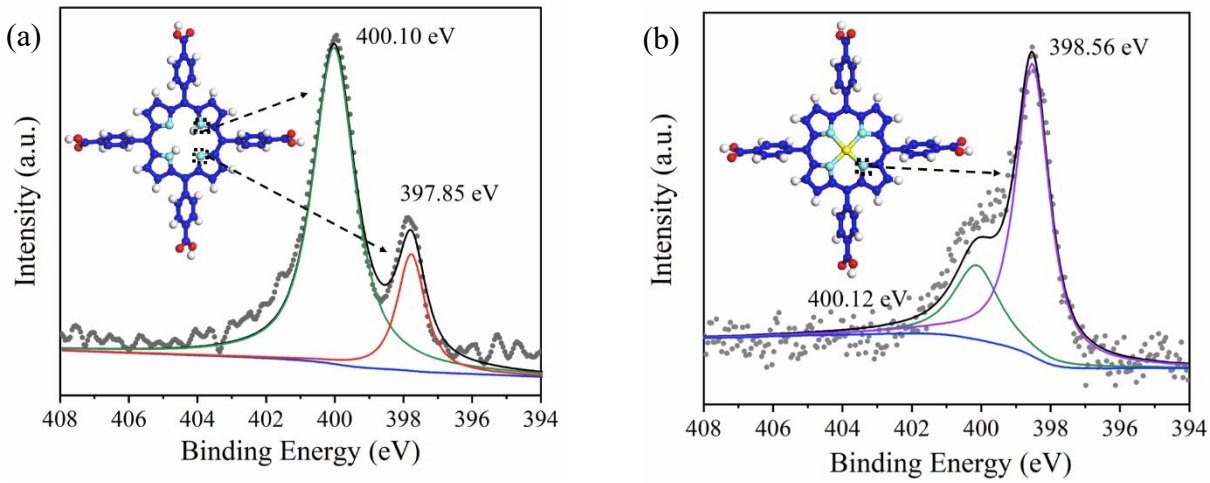

Figure S1. XPS N 1s spectra **(a)** before the implantation of Cu (TCPP@P25); **(b)** after the implantation of Cu (TCPP-Cu@P25).

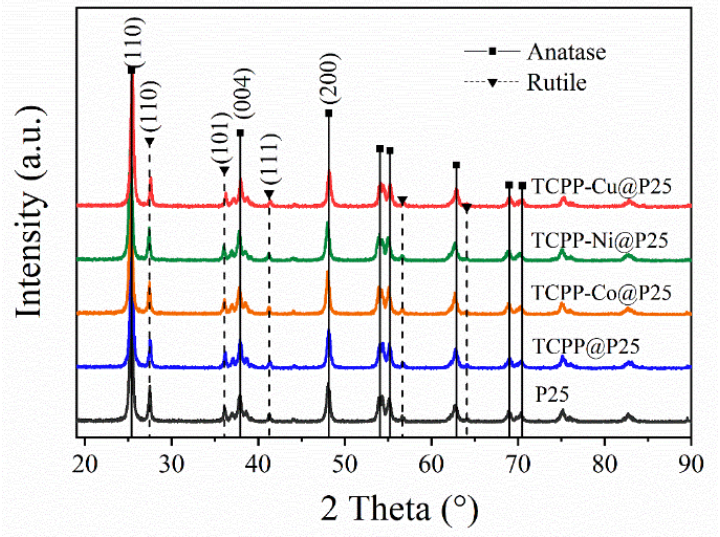

Figure S2. XRD pattern for P25 and prepared samples: TCPP@P25 and TCPP-M (M=Co, Ni, Cu) @P25.

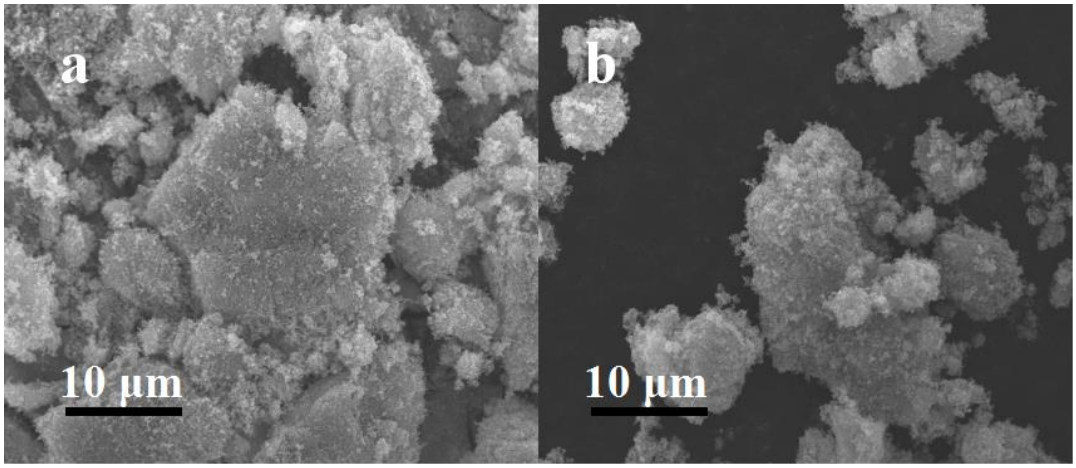

Figure S3. SEM images of (a) P25 and (b) TCPP-Cu@P25.

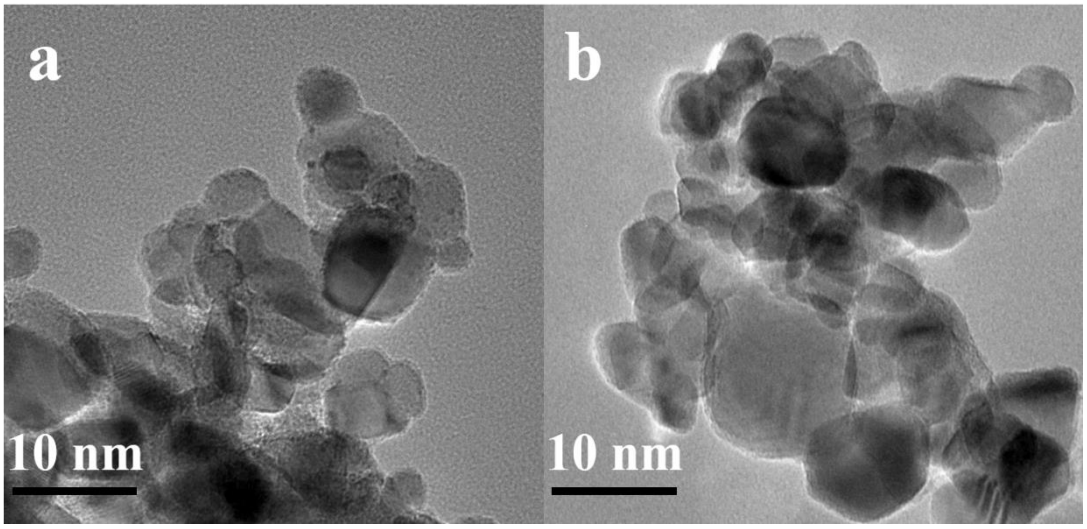

Figure S4. TEM images of (a) P25 and (b) TCPP-Cu@P25 at low magnification.

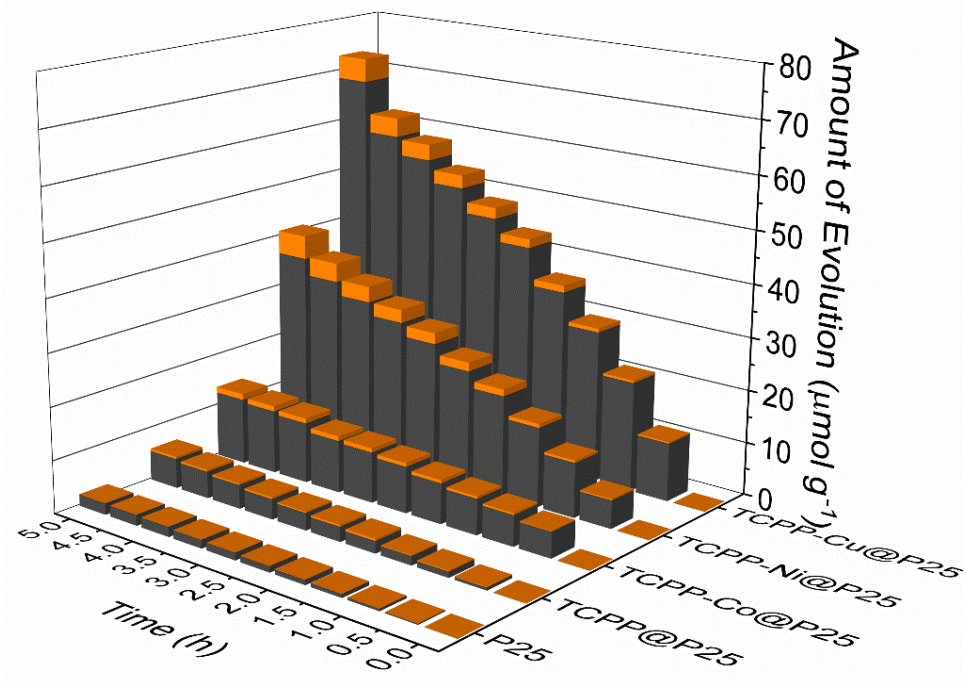

Figure S5. Time dependent of CO and CH_4 evolution over P25, TCPP@P25, TCPP-Co@P25, TCPP-Ni@P25 and TCPP-Cu@P25.

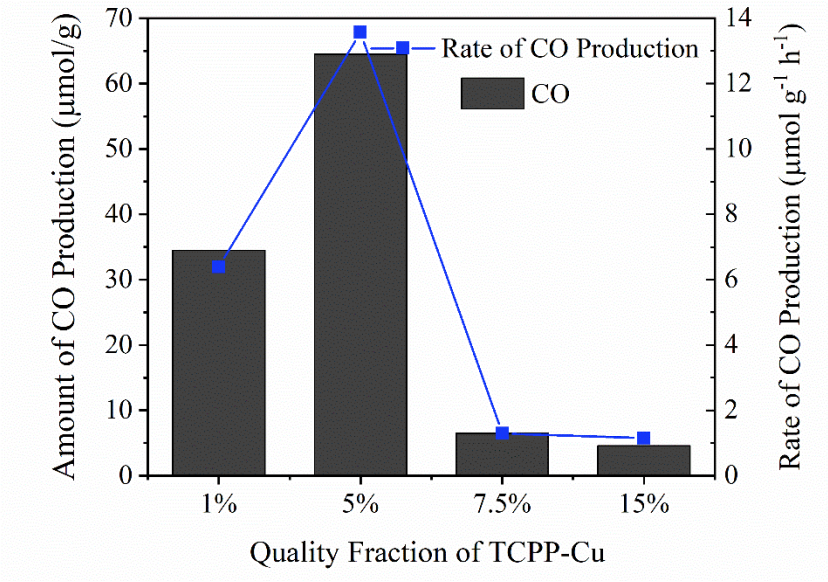

Figure S6. Photocatalytic CO production performance over TCPP-Cu@P25 with different cocatalyst mass fraction.

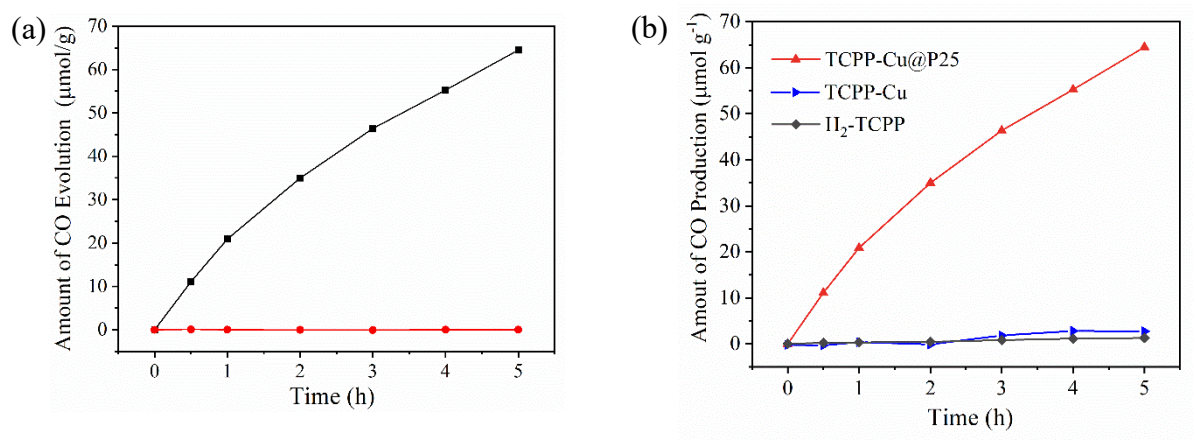

Figure S7. Time course of CO evolution **(a)** with (black line) and without (red line) L42 filter; **(b)** over TCPP-Cu@P25, H_2-TCPP ligand and TCPP-Cu complex (the other experimental conditions were identical to those in Fig. 1d).

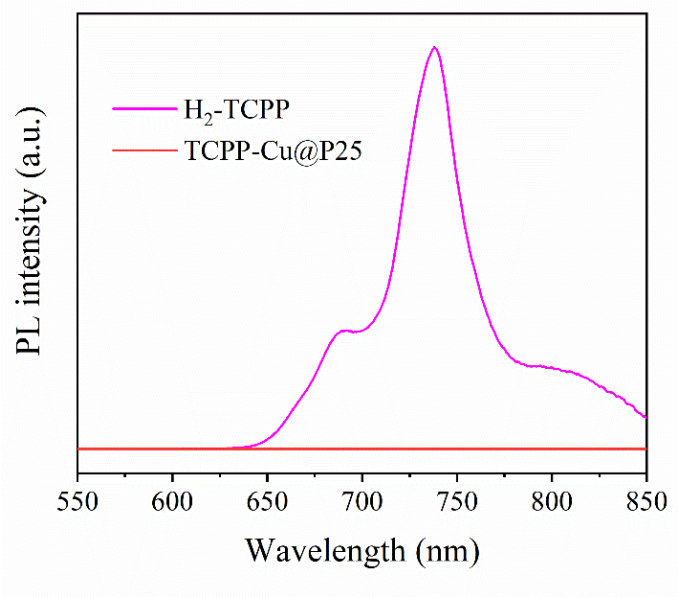

Figure S8. PL spectra over TCPP-Cu@P25 and H_2TCPP ligand in the range of porphyrin fluorescence peak. After coupling with P25, the porphyrin fluorescence peak could not be observed.

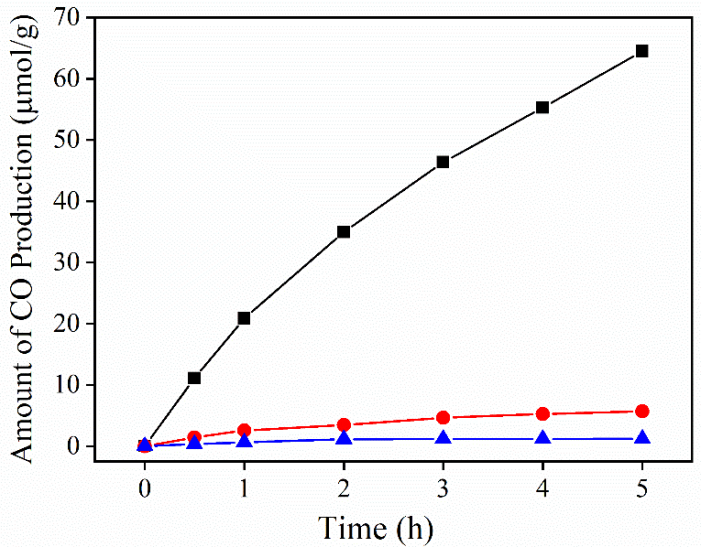

Figure S9. Time dependent of CO yield TCPP-Cu@P25 under different conditions: with CO_2 gas and deionized water (black); with Ar gas and deionized water (red); with CO_2 gas but without water (blue), other conditions remain the same with Fig. 1d.

Table S1. Relative quantitative analysis of O 1s in the XPS spectra of TCPP@P25 and TCPP-Cu@P25 before (B.R.) and after (A.R.) the photoreduction reaction.

O 1s	B.R.	A.R.
TCPP@P25	47.16%	49.31%
TCPP-Cu@P25	41.70%	46.54%

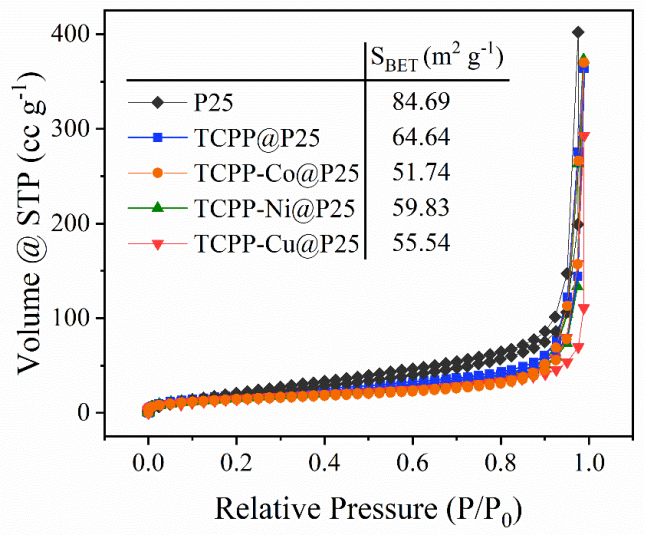

Figure S10. N_2 adsorption and desorption curves and BET surface areas of P25, TCPP@P25 and TCPP-M (M=Co, Ni, Cu) @P25.

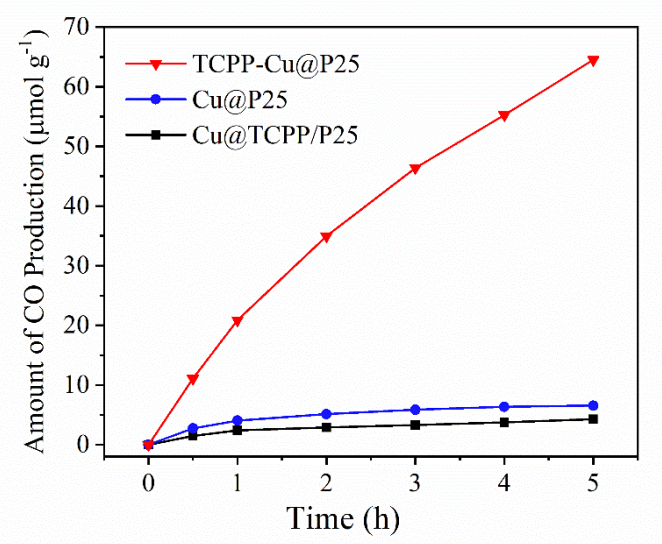

Figure S11. Time course of CO yield over TCPP-Cu@P25, Cu@P25 (photodeposited Cu on P25) and Cu@TCPP/P25 (photodeposited Cu on TCPP@P25).